Electronic Supplementary Material (ESI) for New Journal of Chemistry.

Supplementary Data

Calix[4]arene-based polyoxometalate organic-inorganic hybrid and coordination polymer as heterogeneous catalysts for azide-alkyne cycloaddition and Knoevenagel condensation reaction

Liu-Juan Yue,[a] Ying-Ying Liu,[a,*] Guo-Hai Xu,[b,*] and Jian-Fang Ma[a,*]

Material and Methods.

All chemicals were purchased from merchants and were employed directly without any purification. Powder X-ray diffraction (PXRD) patterns were detected on a Rigaku Dmax 2000 X-ray diffractometer with graphite monochromatized CuKα radiation (λ = 0.154 nm). IR spectra were measured by an Alpha Centaurt FT/IR spectrophotometer. Elemental analysis (C, H and N) were carried out on a Euro vector EA3000 analyzer. The conversion yields of catalytic reactions were calculated by GC which equip with capillary (30 m long × 0.25 mm i.d., WondaCap 17) and FID detector (GC-2014C, Shimadzu, Japan), and further confirmed by ^{1}H NMR spectra which were detected in $CDCl_3$ on a Bruker 600 MHz. ICP data were collected from a Leeman laboratories prodigy inductively coupled plasma-optical atomic emission spectrometer (ICP-AES).

X-ray Crystallography.

Crystallographic data for **1** and **2** were collected on an Oxford Diffraction Gemini R CCD with graphite monochromated MoKα radiation (λ = 0.71073 Å) at 293 K. Absorption correction was carried out with a multiscan technique. The structures were solved by direct methods with SHELXS-18 and refined on F^2 by full-matrix least-squares employing SHELXTL-2018 within WINGX. The SQUEEZE function refinement was utlized because of the disordered solvents for **1**.[1] The disordered C19, C20, C29, C31 and C68 atoms in **1**; C57, C58, C59, C60,C68, C69, C70 and C71 atoms in **2** was refined by splitting over two sites, with a total occupancy of 1. The maxima and minima residual electron density for **1** are 3.85 and -4.21, respectively. One of which locates 1.28Å from Cu2, three of which keep free, and others are locate around the POMs. Unfortunately, we did not obtain satisfactory crystallographic data for **1**. The poor data maybe caused by its crystal quality. Crystallographic data are given in Table S1. Selected bond lengths and bond angles are listed in Tables S2.

Table S1 Crystal data and structure refinements.

	1	**2**
Formula	$C_{70}H_{83}N_5O_{26}Si_{0.5}W_6Cu_2$	$C_{70}H_{79}CdN_5O_4Cl_2$
Mr	2654.64	1237.68
Crystal system	Triclinic	Orthorhombic
Space group	*P*-1	*Pbna*
a (Å)	11.9741(6)	13.1543(5)
b (Å)	12.1625(8)	24.6370(8)
c (Å)	28.3572(14)	42.2769(16)
α (°)	85.192(5)	90
β (°)	88.211(4)	90
γ (°)	72.490(5)	90
V (Å^3)	3924.5(4)	13701.2(9)
Z	2	8
D_{calc} (g cm^{-3})	2.246	1.200
F(000)	2510	5184.0
R_{int}	0.0965	0.0352
GOF on F^2	1.0520	1.032
$R1^a$[I >2σ(I)]	0.0951	0.0413
wR_2^b(all data)	0.2706	0.1039

$^aR_1 = \Sigma||F_o| - |F_c||/\Sigma|F_o|$. $^bwR_2 = \{\Sigma[w(F_o^2-F_c^2)^2]/\Sigma w(F_o^2)^2]\}^{1/2}$.

Table S2 Selected bond distances (Å) and angles (deg) for **1** and **2.**

1			
Cu(1)-N(2)$^{\#1}$	1.864(17)	Cu(2)-N(4)	1.880(16)
Cu(1)-N(1)	1.88(2)	N(2)$^{\#1}$-Cu(1)-N(1)	168.3(8)
Cu(2)-N(3)$^{\#2}$	1.846(14)	N(3)$^{\#2}$-Cu(2)-N(4)	165.1(8)

Symmetry codes: $^{\#1}$ x, y+1, z; $^{\#2}$ -x+1, -y+1, -z+2

2			
Cd(1)-N(4)	2.390(2)	N(2)-Cd(1)-Cl(1)	94.46(6)
Cd(1)-N(2)	2.398(2)	N(1)-Cd(1)-Cl(1)	92.35(5)
Cd(1)-N(1)	2.4268(14)	N(4)-Cd(1)-Cl(2)	86.73(6)
Cd(1)-Cl(1)	2.4856(7)	N(2)-Cd(1)-Cl(2)	86.99(6)
Cd(1)-Cl(2)	2.6356(7)	N(1)-Cd(1)-Cl(2)	88.64(4)
Cd(1)-Cl(2)$^{\#1}$	2.6379(7)	Cl(1)-Cd(1)-Cl(2)	178.31(3)
N(4)-Cd(1)-N(2)	172.47(8)	N(4)-Cd(1)-Cl(2)$^{\#1}$	92.51(5)
N(4)-Cd(1)-N(1)	90.54(7)	N(2)-Cd(1)-Cl(2)$^{\#1}$	91.15(6)
N(2)-Cd(1)-N(1)	85.17(7)	N(1)-Cd(1)-Cl(2)$^{\#1}$	173.41(4)
N(4)-Cd(1)-Cl(1)	91.89(6)	Cl(1)-Cd(1)-Cl(2)$^{\#1}$	93.39(3)
Cl(2)-Cd(1)-Cl(2)$^{\#1}$	85.70(2)		

Symmetry codes: $^{\#1}$ -x, -y, -z.

The procedure includes two major steps:[2]

Under nitrogen protection, 50 g (0.333 mol) *p*-tert-butylphenol, 32 mL 36％ (0.384mo1) aqueous formaldehyde solution and 5 mL 3.45mol/L sodium hydroxide solution were added to a 1000 mL three-necked bottle. Then, the mixture was stirred and heated at 120°C for 2 h. After cooling to RT, 500 mL of diphenyl ether was added and heated for a further 2 hours. Then cooling to RT, 500 mL of ethyl acetate was added, and a precipitate appeared immediately, stirred for 30 minutes. The solid product was filtered, washed by ethyl acetate and acetic acid to give a yellowish crude. Recrystallized with toluene, intermediate product *p*-tert-butylcalix(4)arene was obtained (yield 75%).

Secondly, *p*-tert-butylcalix(4)arene (3.85 mmol) and sodium hydride (129 mmol) were suspended in a mixture of dried DMF, the mixture was stirred for 40 min, then 3-chloromethyl pyridine hydrochloride (42.9 mmol) was added. The mixture was placed in a water bath and heated at 50 °C for 48 h. After the reaction was completed, 500 mL of water was added to the flask, and the mixture was stirred for 30 min. The solvent was removed by rotary evaporation, and the solid was dried at 80°C then recrystallized by acetone. Finally, white solid L was obtained in a yield of 57.2% (2.22g).

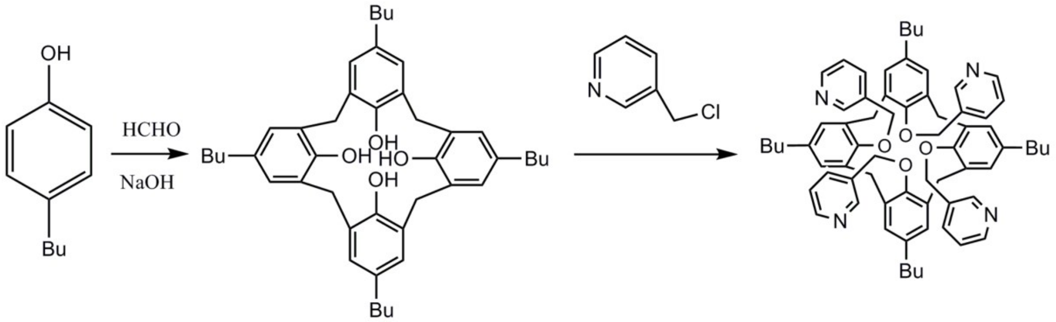

Scheme S1 Schematic synthesis of ligand L.

1 A. L. Spek, *Acta Crystallogr. Se*ct. *C: Struct. Chem*. **2015**, *71*, 9-18.

2 A. F. Danil de Namor, F. J. Sueros Velarde and M. C. Cabaleiro, *Polyhedron, 1997,* ***16****, 1885−1888.*

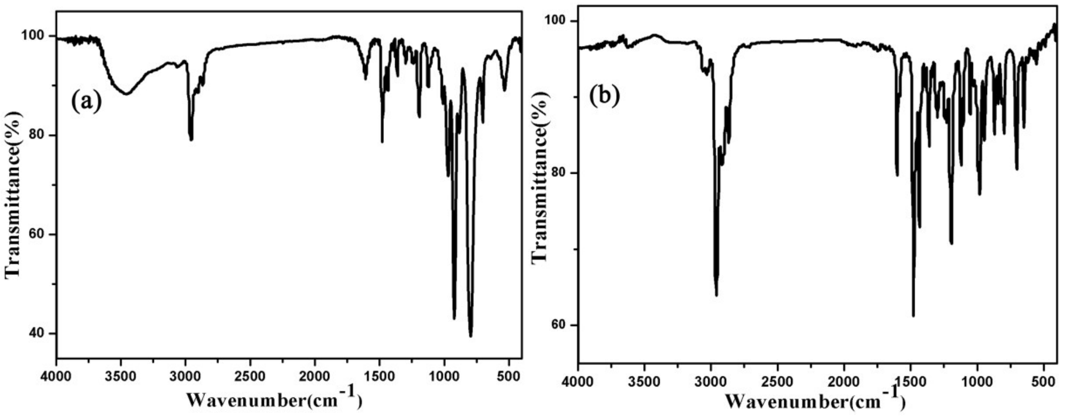

Fig. S1 FT-IR spectra for **1** (a) and **2** (b).

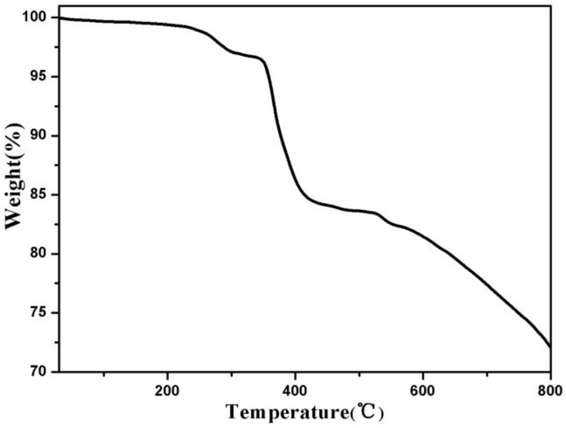

Fig. S2 Thermogravimetric curve of **1.**

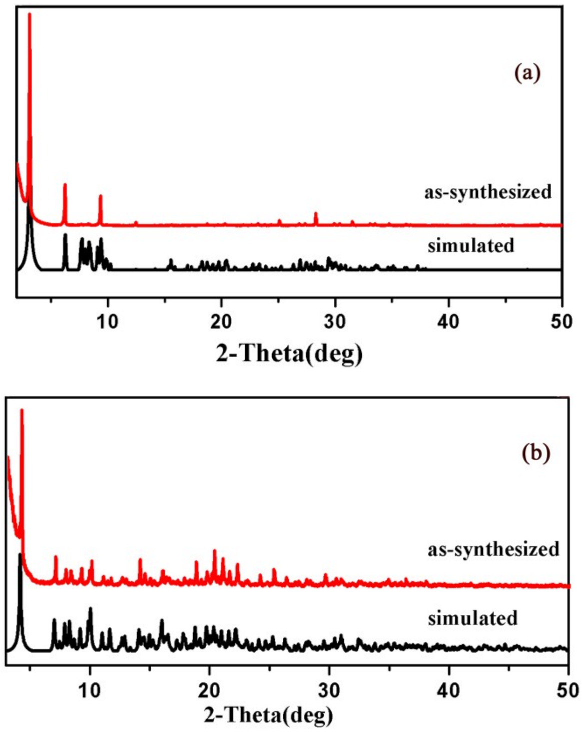

Fig. S3 PXRD patterns of **1** (a) and **2** (b) simulated (black), experimental (red).

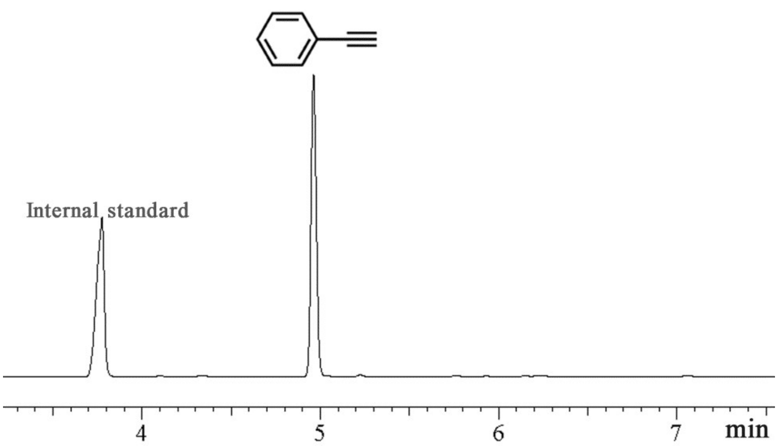
Internal standard
4
5
6
7
min

(a)

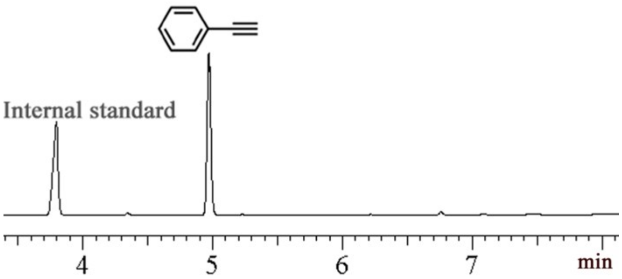
Internal standard
4
5
6
7
min

(b)

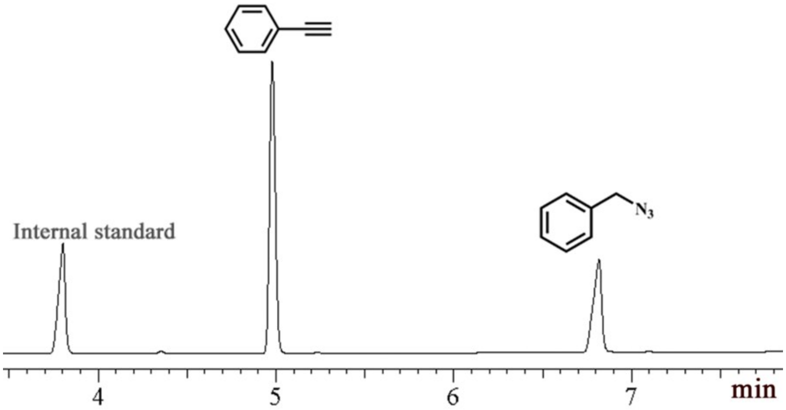
Internal standard
N3
4
5
6
7
min

(c)

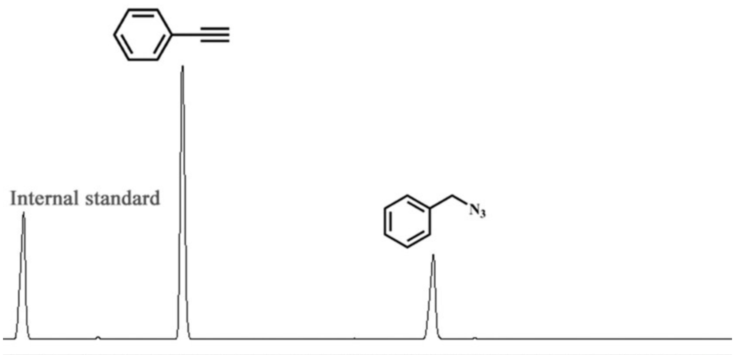
Internal standard
N3
4
5
6
7
8
min

(d)

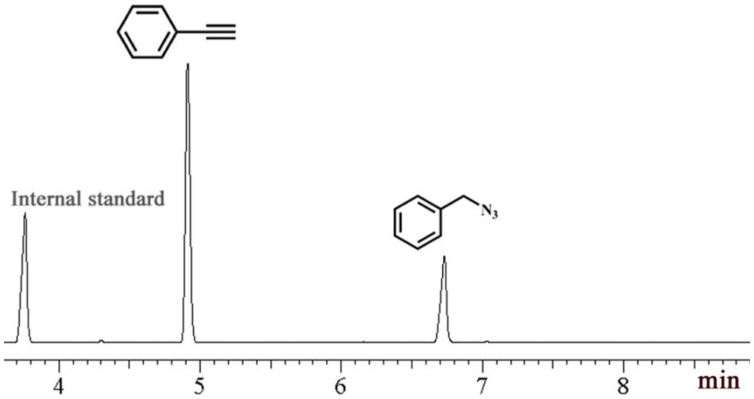
Internal standard
N3
4
5
6
7
8
min

(e)

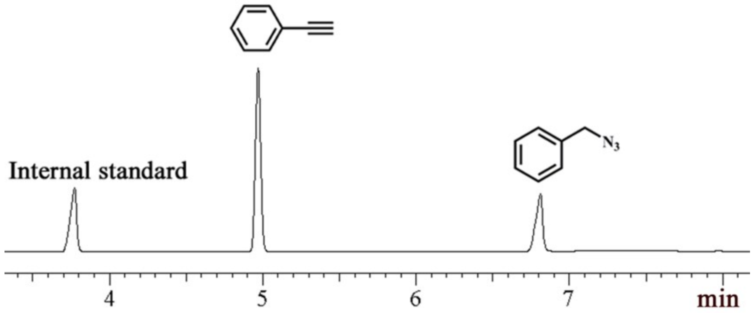
Internal standard
N3
4
5
6
7
min

(f)

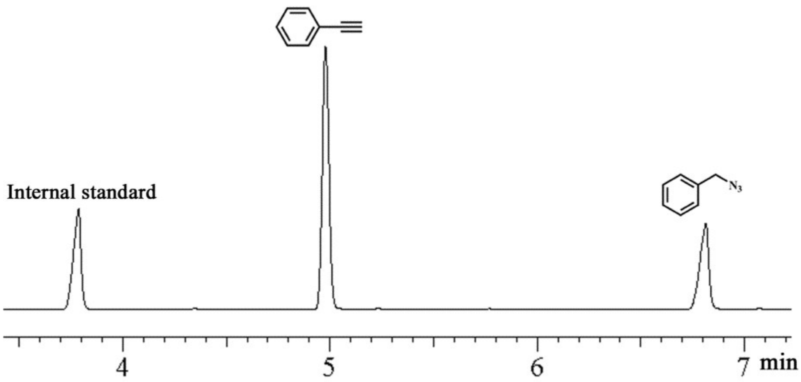
Internal standard
N3
4
5
6
7
min

(g)

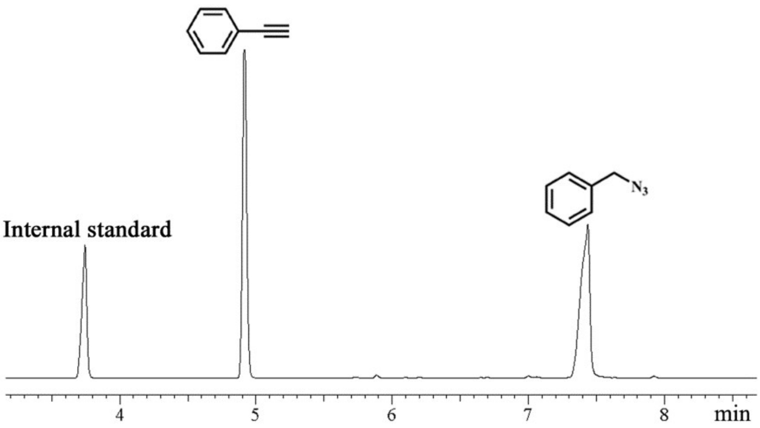
Internal standard
N3
4
5
6
7
8
min

(h)

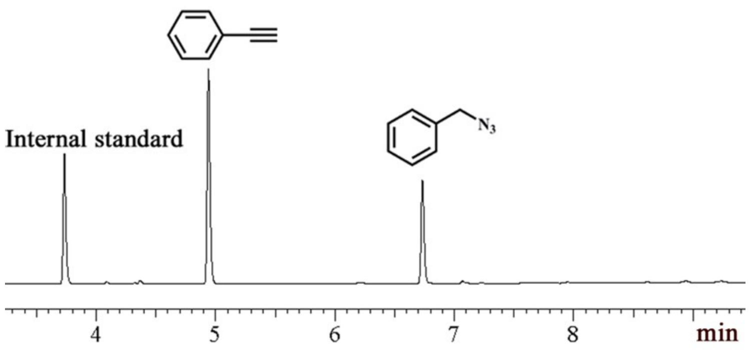
Internal standard
N3
4
5
6
7
8
min

(i)

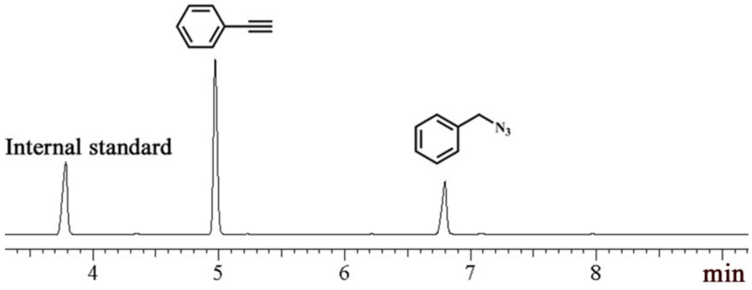
Internal standard
N3
4
5
6
7
8
min

(j)

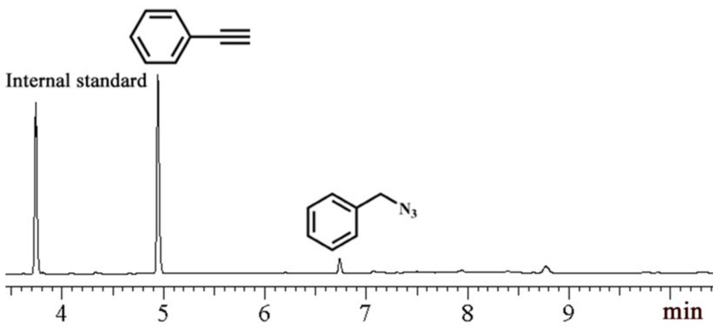
Internal standard
N3
4
5
6
7
8
9
min

(k)

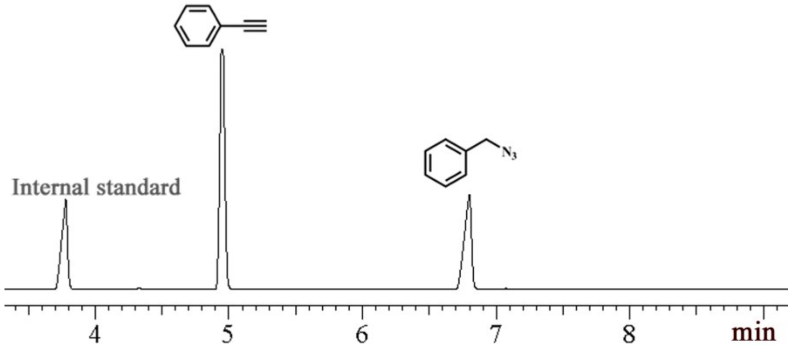
Internal standard
N3
4
5
6
7
8
min

(l)

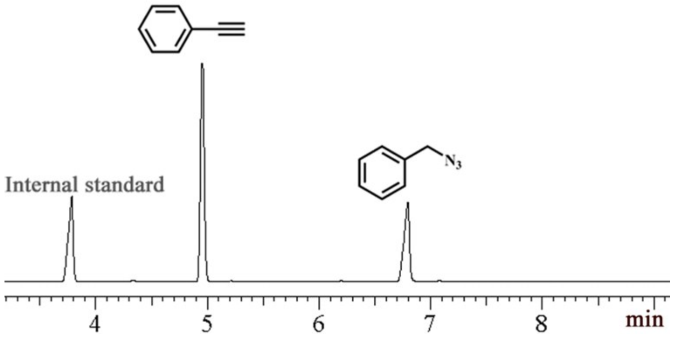

(m)

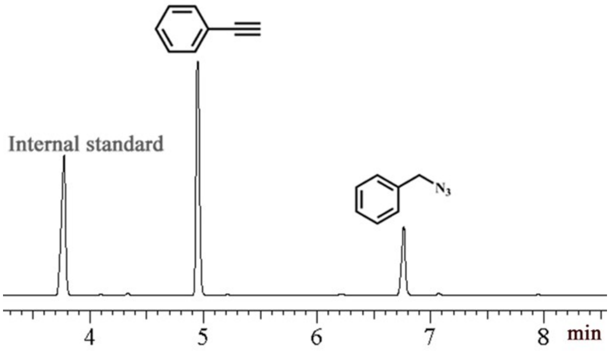

(n)

Fig. S4 GC spectra of catalytic reactions between the benzyl azide and phenylacetylene under various conditions. (a) **1** (20 mg), CH_3OH as solvent for 10 hours at 70°C. (b) **1** (20 mg), CH_3CH_2OH as solvent for 10 hours at 70°C. (c) **1** (20 mg), CH_3CN as solvent for 10 hours at 70°C. (d) **1** (20 mg), CH_2Cl_2 as solvent for 10 hours at 70°C. (e) **1** (20 mg), $C_6H_5CH_3$ as solvent for 10 hours at 70°C. (f) **1** (0 mg), CH_3OH as solvent for 10 hours at 70°C. (g) CuCl (0.75 mg) as catalyst, CH_3OH as solvent for 10 hours at 70°C. (h) $H_4SiW_{12}O_{40}$ (10.8 mg) as catalyst, CH_3OH as solvent for 10 hours at 70°C. (i) **1** (5 mg), CH_3OH as solvent for 10 hours at 70°C. (j) **1** (10 mg), CH_3OH as solvent for 10 hours at 70°C. (k) **1** (15 mg), CH_3OH as solvent for 10 hours at 70°C. (l) **1** (20 mg), CH_3OH as solvent for 12 hours at room temperature. (m) **1** (20 mg), CH_3OH as solvent for 12 hours at 40°C. (n) **1** (20 mg), CH_3OH as solvent for 12 hours at 60°C.

Table S3 The effects of time and catalysts on AAC reaction.

Entry	Catalyst (mg)	Temperature (℃)	Solvent	Time (h)	conversion(%) (with catalyst)	conversion(%) (without catalyst)

1	20	70	MeOH	2	26%	26%
2				4	52%	26%
3				6	85%	27%
4				8	94%	27%
5				10	98%	29%

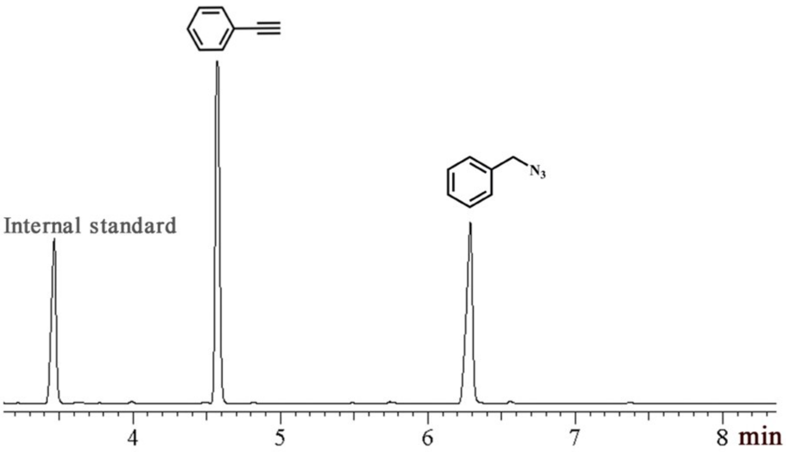

(a)

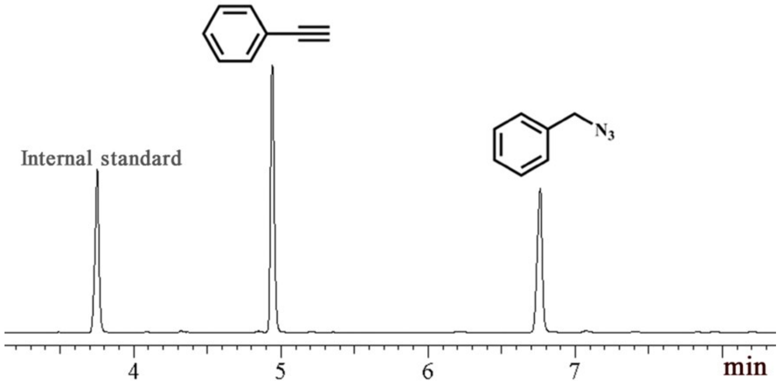

(b)

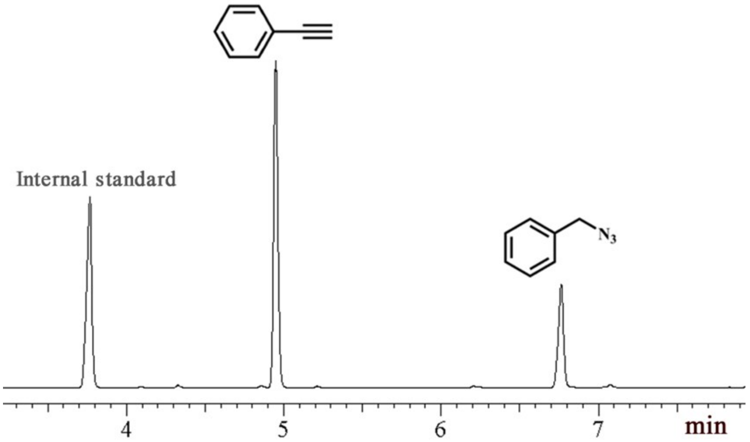

(c)

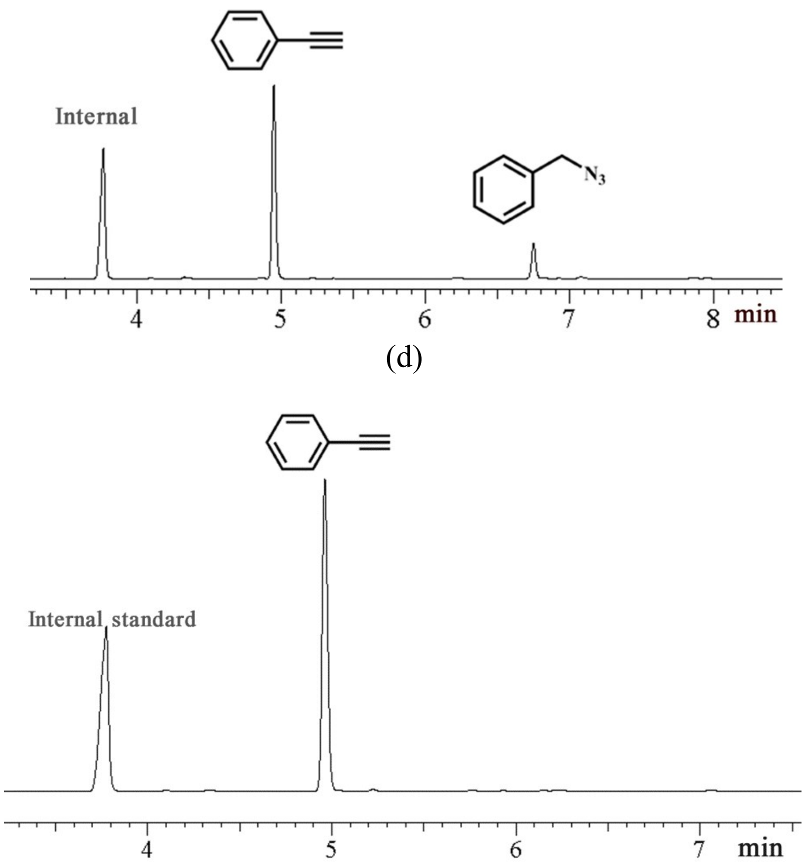

(d)

(e)

Fig. S5 GC spectra of catalytic reactions between the benzyl azide and phenylacetylene at different reaction time. (a) Catalytic reaction for 2 hours. (b) Catalytic reaction for 4 hours. (c) Catalytic reaction for 6 hours. (d) Catalytic reaction for 8 hours. (e) Catalytic reaction for 10 hours.

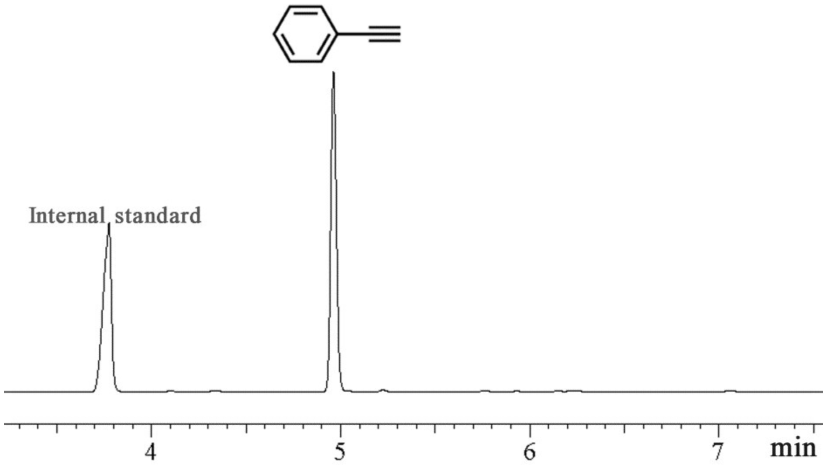

(a)

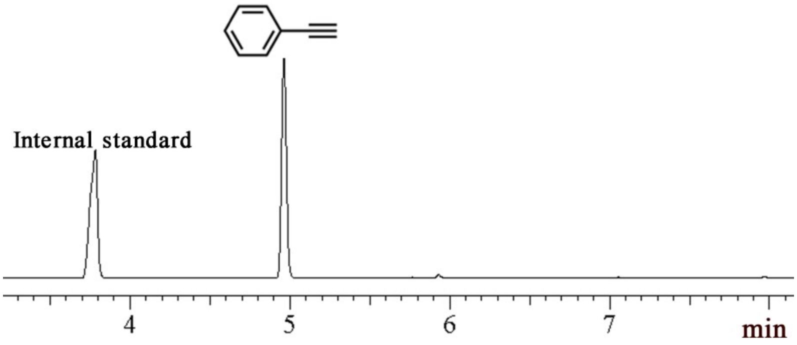
Internal standard
4
5
6
7
min

(b)

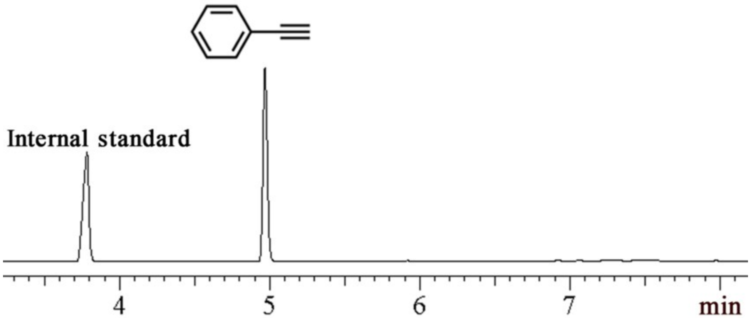
Internal standard
4
5
6
7
min

(c)

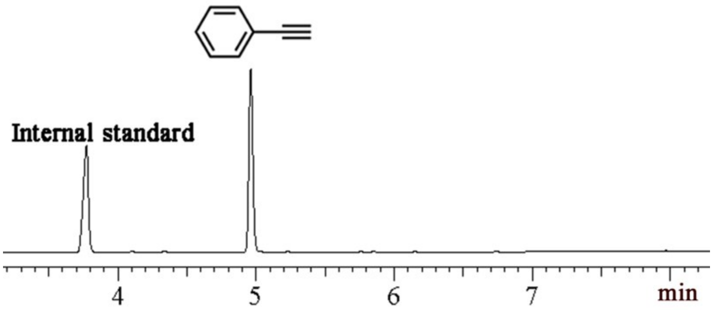
Internal standard
4
5
6
7
min

(d)

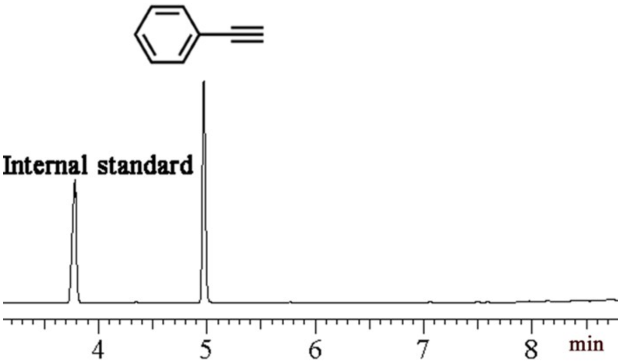
Internal standard
4
5
6
7
8
min

(e)

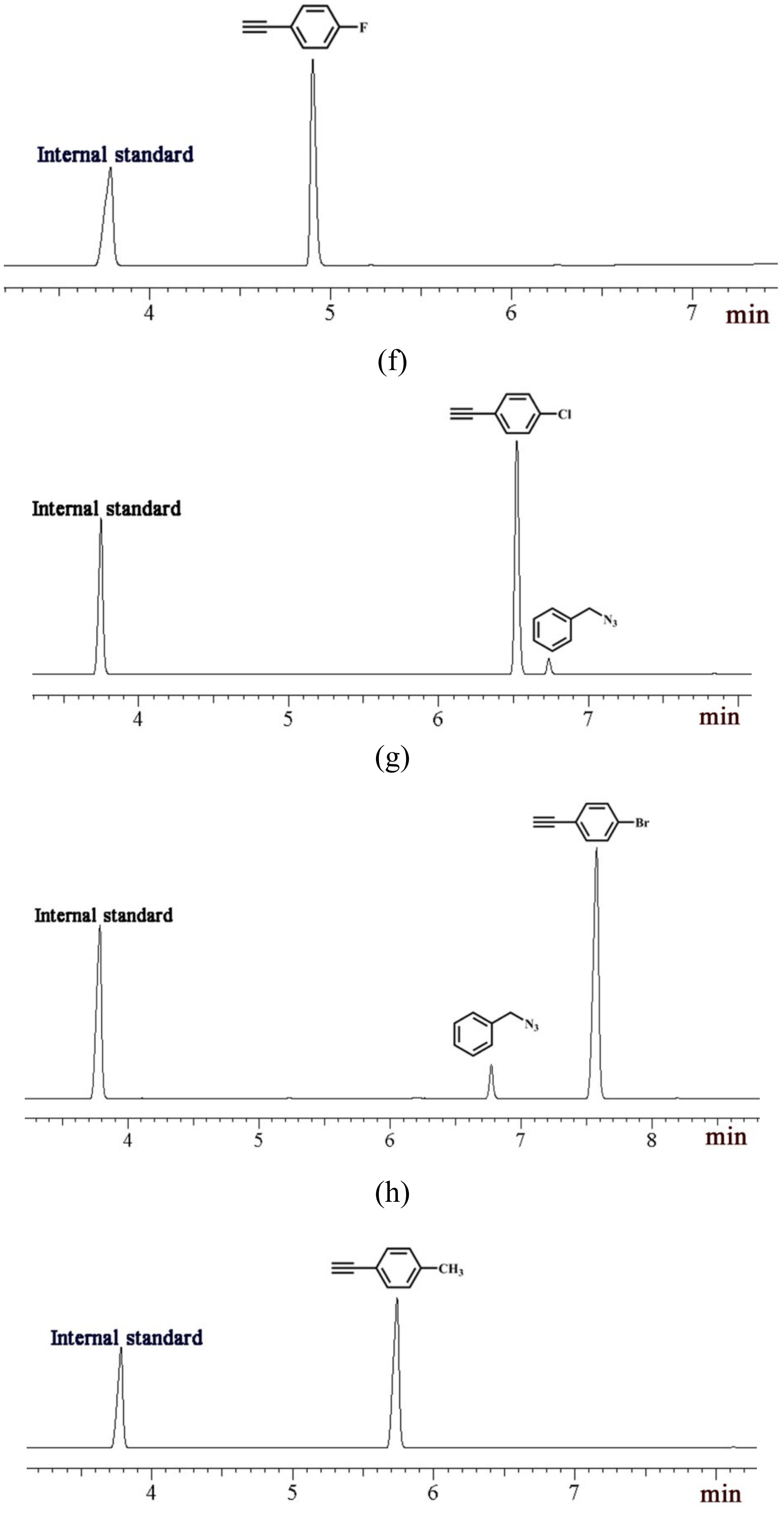

(f)

(g)

(h)

(i)

Fig. S6 GC spectra for the catalytic reactions between substituted benzyl azides and phenylacetylenes with different groups under same conditions (20 mg of **1**, CH_3OH and 70 °C). (a) Catalytic rectioans of (azidomethyl)benzene. (b) 1-(azidomethyl)-4-

methylbenzene and phenylacetylene. (c) 1-(azidomethyl)-3-methylbenzene and phenylacetylene. (d) 1-(azidomethyl)-2-fluoro benzene and phenylacetylene. (e) 1-(azidomethyl)-4-nitrobenzene and phenylacetylene. (f) 1-(azidomethyl)benzene and 1-ethynyl-4-fluorobenzene. (g) 1-(azidomethyl)benzene and 1-ethynyl-4-chlorobenzene. (h) 1-(azidomethyl)benzene and 1-ethynyl-4-bromobenzene. (i) 1-(azidomethyl)benzene and 1-ethynyl-4-methylbenzene.

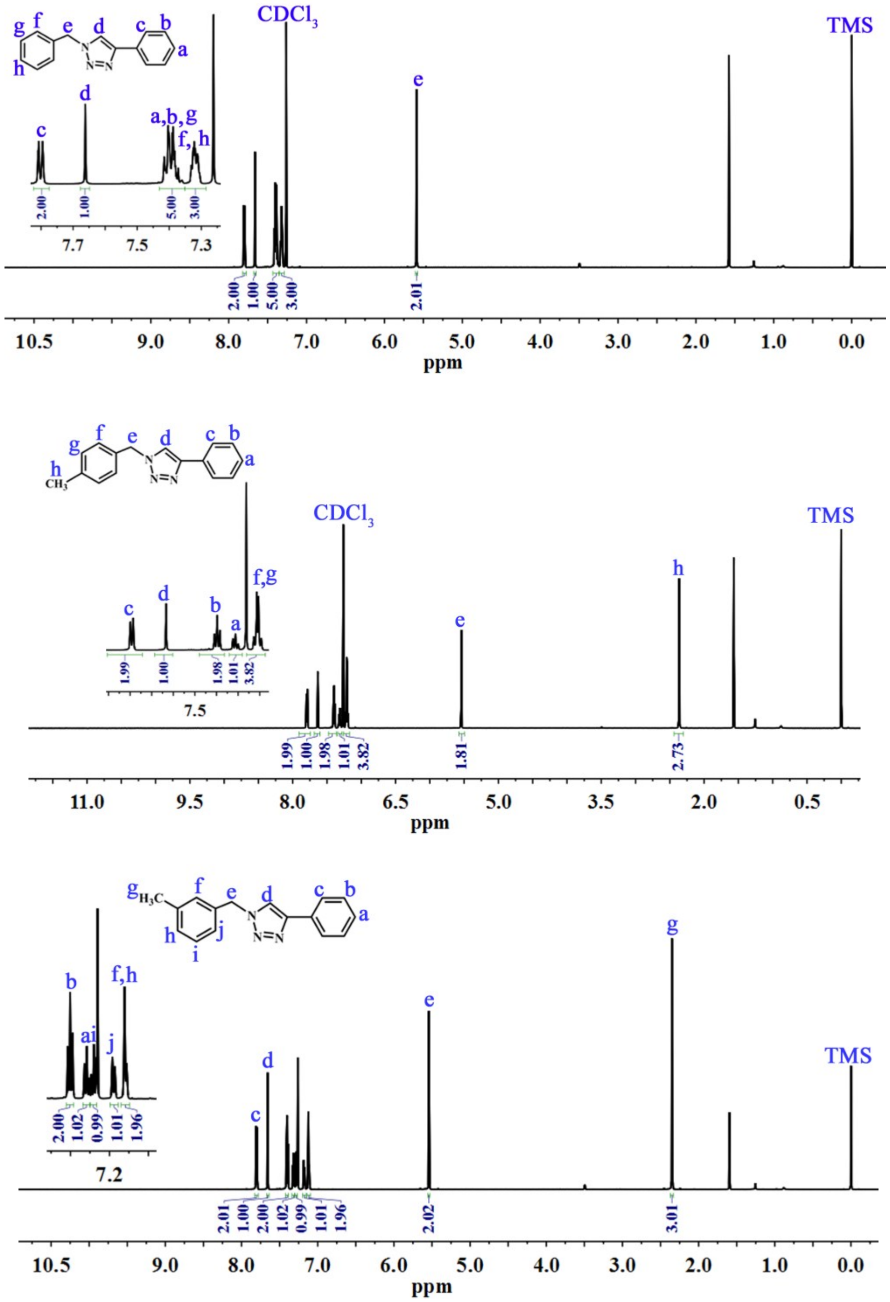

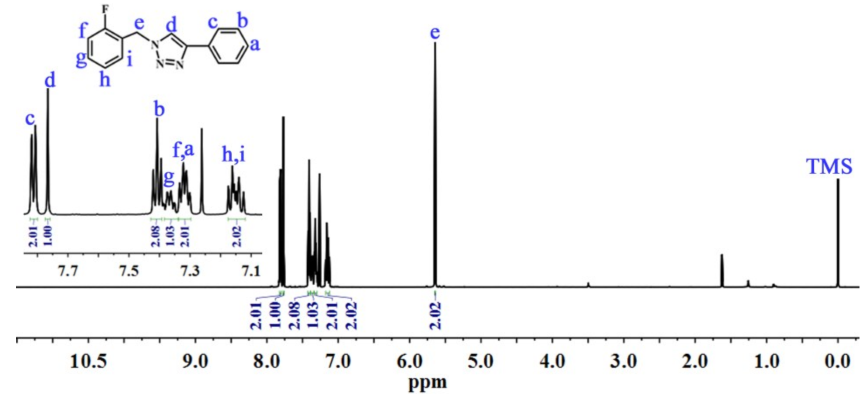
F
f
e
d
c
b
a
g
i
h
N
N=N
d
c
b
g
f,a
h,i
2.01
1.00
2.08
1.03
2.01
2.02
7.7
7.5
7.3
7.1
e
TMS
2.01
1.00
2.08
1.03
2.01
2.02
2.02
10.5
9.0
8.0
7.0
6.0
5.0
4.0
3.0
2.0
1.0
0.0
ppm

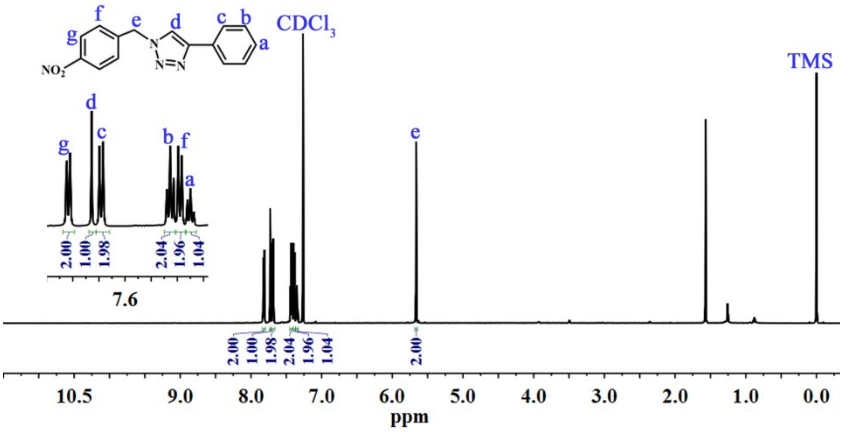
g
f
e
d
c
b
a
NO2
N
N=N
CDCl3
TMS
d
g
c
b
f
a
e
2.00
1.00
1.98
2.04
1.96
1.04
7.6
2.00
1.00
1.98
2.04
1.96
1.04
2.00
10.5
9.0
8.0
7.0
6.0
5.0
4.0
3.0
2.0
1.0
0.0
ppm

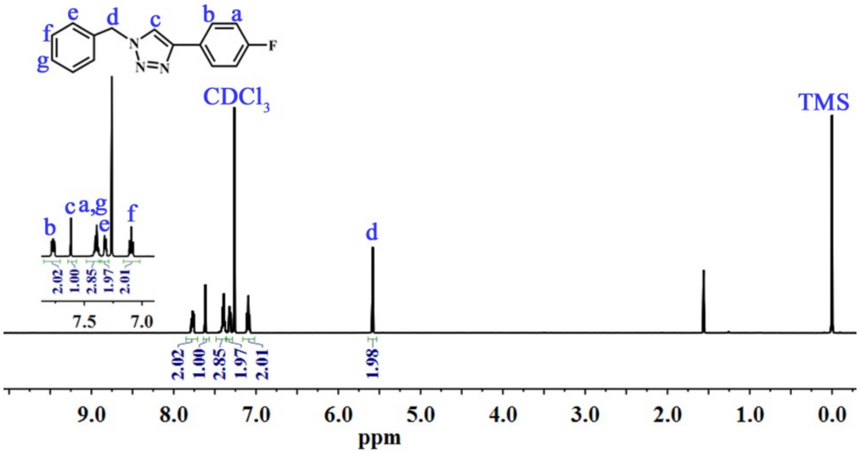
e
d
c
b
a
f
g
F
N
N=N
CDCl3
TMS
b
c
a,g
e
f
2.02
1.00
2.85
1.97
2.01
7.5
7.0
d
2.02
1.00
2.85
1.97
2.01
1.98
9.0
8.0
7.0
6.0
5.0
4.0
3.0
2.0
1.0
0.0
ppm

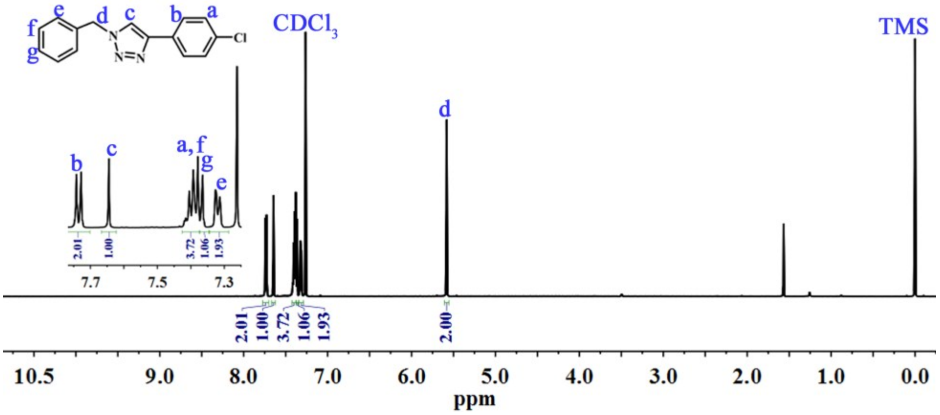
e
d
c
b
a
f
g
Cl
N
N=N
CDCl3
TMS
d
b
c
a,f
g
e
2.01
1.00
3.72
1.06
1.93
7.7
7.5
7.3
2.01
1.00
3.72
1.06
1.93
2.00
10.5
9.0
8.0
7.0
6.0
5.0
4.0
3.0
2.0
1.0
0.0
ppm

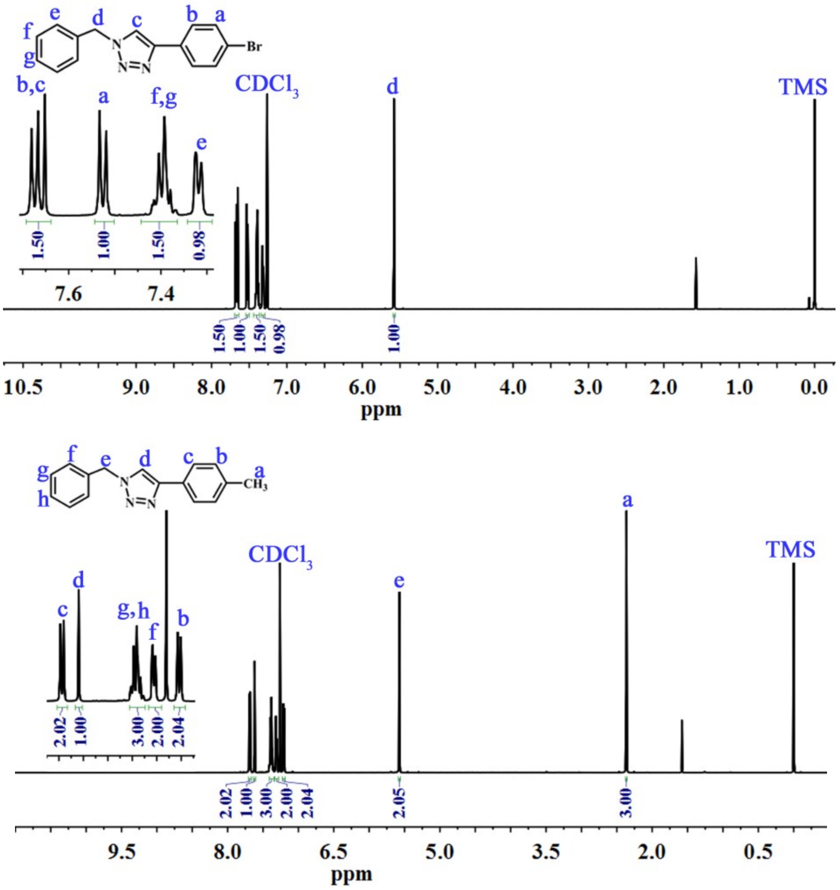

Fig. S7 ^{1}H and spectra of the products from AAC reaction (The signals at 1.56 ppm is caused by the impurity H_2O in $CDCl_3$ during the ^{1}H NMR testing).

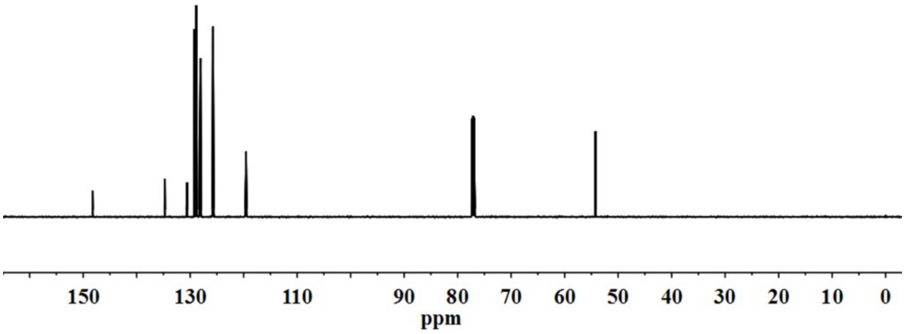

Fig. S8 ^{13}C NMR spectra (600 MHz, $CDCl_3$, TMS) for 1-benzyl-4-phenyl-1H-1,2,3-triazole: δ 54.1, 119.5, 125.6, 127.9, 128.1, 128.7, 129.1, 131.5, 130.5, 134.6, 148.1.

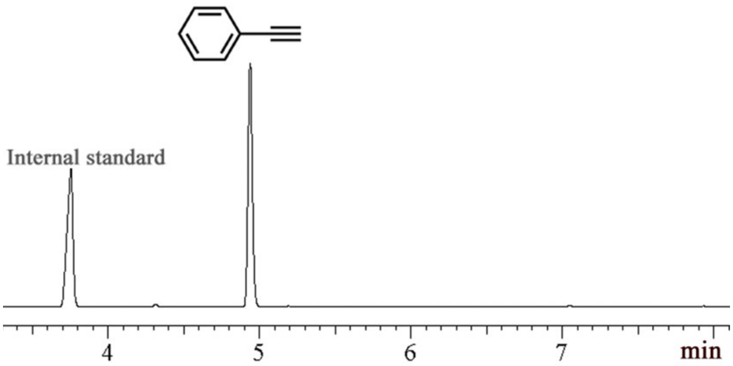
Internal standard
4
5
6
7
min

(a)

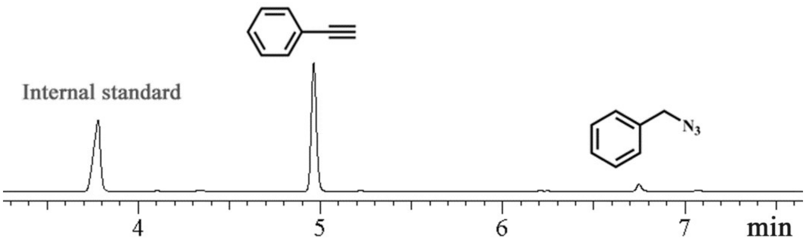
Internal standard
N3
4
5
6
7
min

(b)

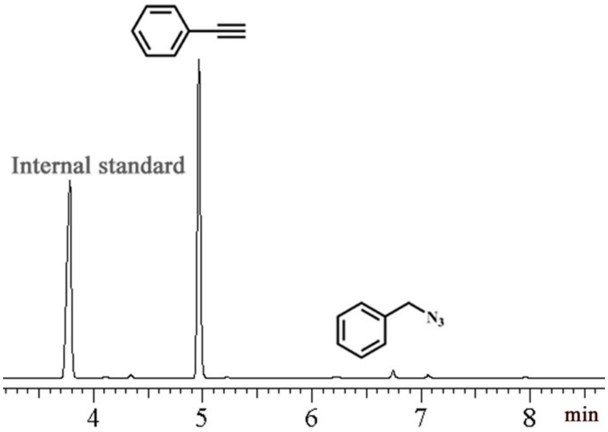
Internal standard
N3
4
5
6
7
8
min

(c)

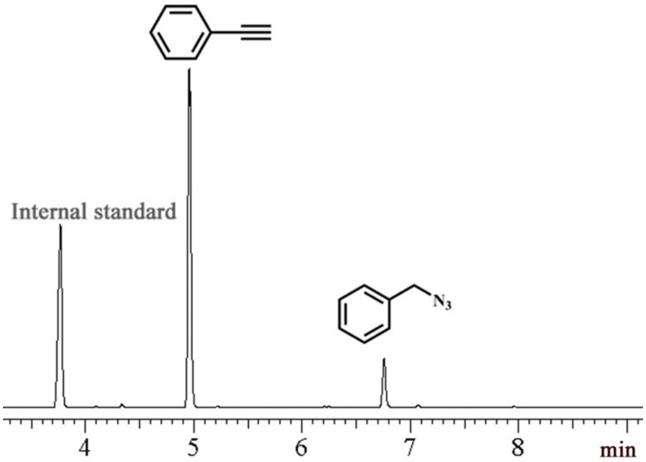
Internal standard
N3
4
5
6
7
8
min

(d)

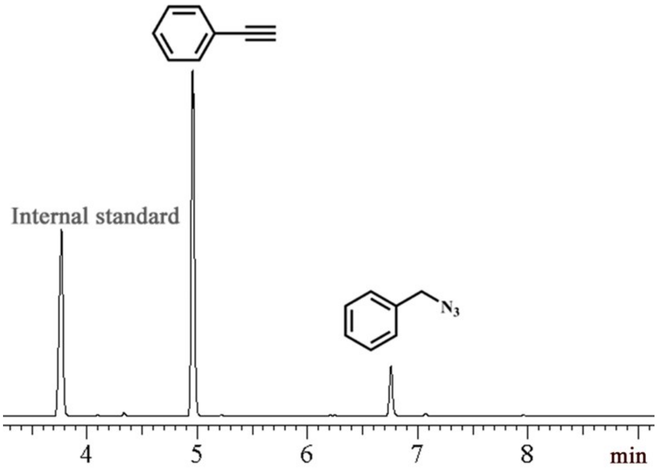

(e)

Fig. S9 GC spectra for the catalytic reactions of benzyl azide and phenylacetylene in different circles. (a) In the first circle. (b) In the second circle. (c) In the third circle. (d) In the fourth circle. (e) In the fifth circle.

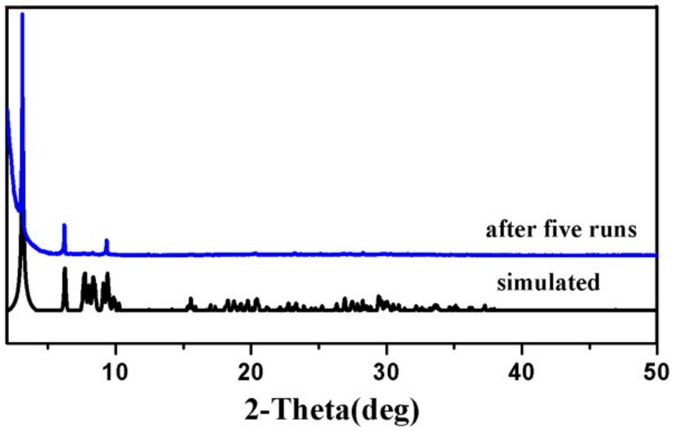

Fig. S10 PXRD patterns of **1** after 5 runs: simulated (black), experimental (blue).

In order to investigate the structural stability during the catalytic reaction, the IR and the solid state UV-Vis spectra of **1** were tested (Figs. S11 and S12). The IR and UV-Vis spectra of **1** after catalysis present good agreements with the spectra before catalytic reaction. The results showed the high stability of **1**.

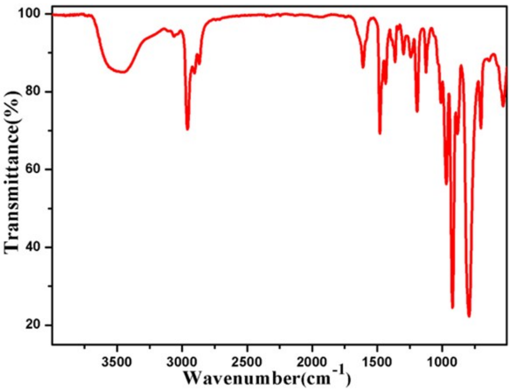

Fig. S11 IR spectra for **1** after catalytic reaction.

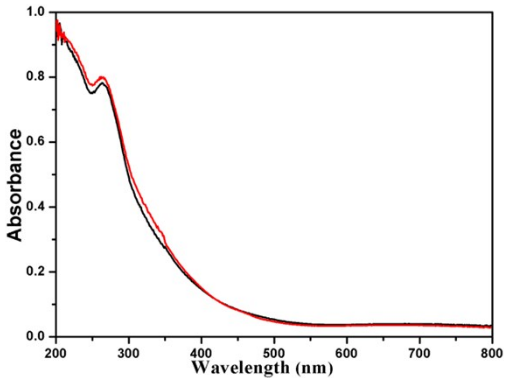

Fig. S12 Solid state UV-Vis spectra of **1** before (black) and after (red) catalytic reaction.

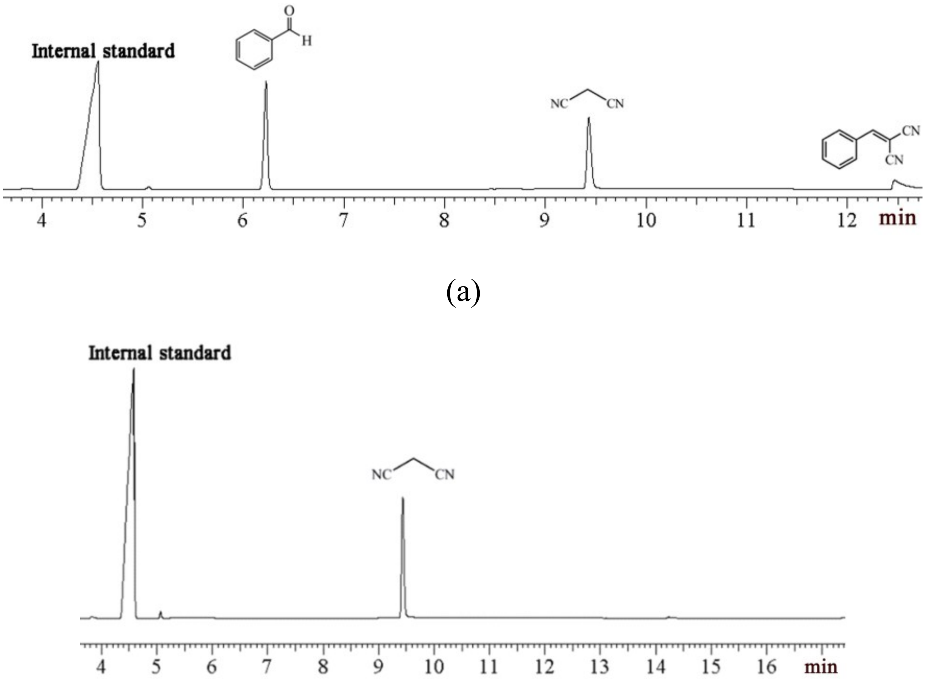

(a)

(b)

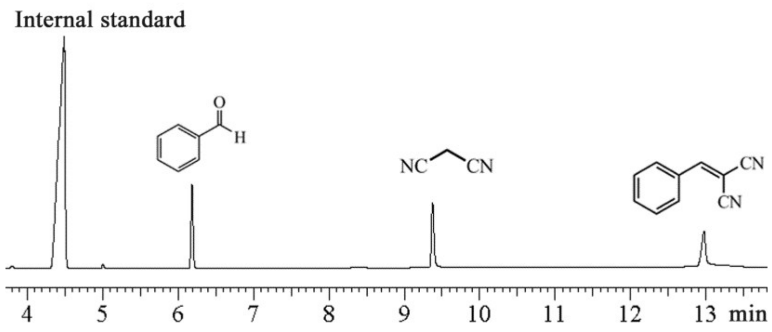
Internal standard
O
H
NC
CN
CN
CN
4
5
6
7
8
9
10
11
12
13
min

(c)

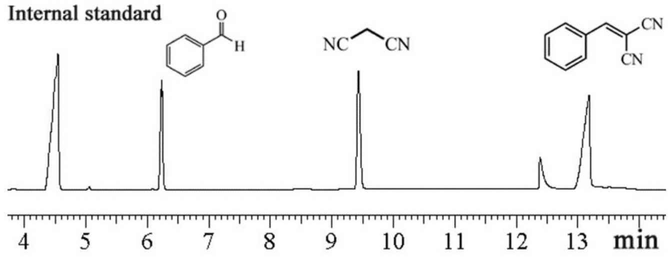
Internal standard
O
H
NC
CN
CN
CN
4
5
6
7
8
9
10
11
12
13
min

(d)

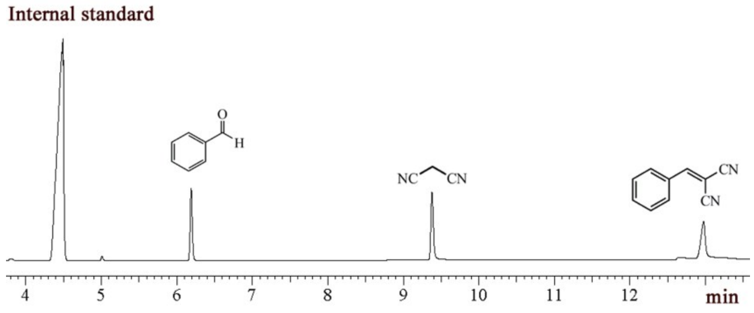
Internal standard
O
H
NC
CN
CN
CN
4
5
6
7
8
9
10
11
12
min

(e)

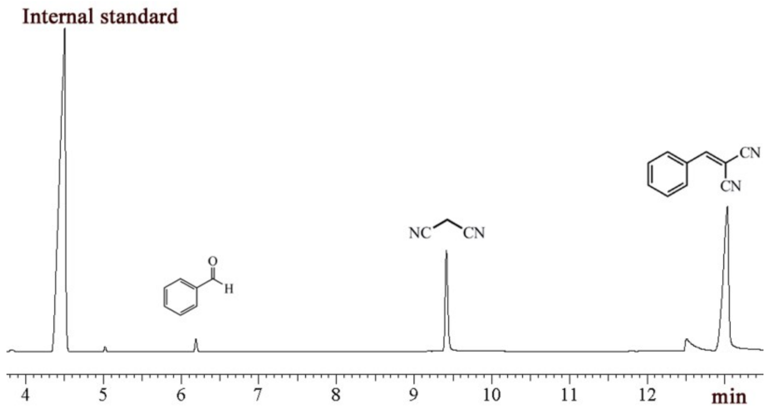
Internal standard
O
H
NC
CN
CN
CN
4
5
6
7
8
9
10
11
12
min

(f)

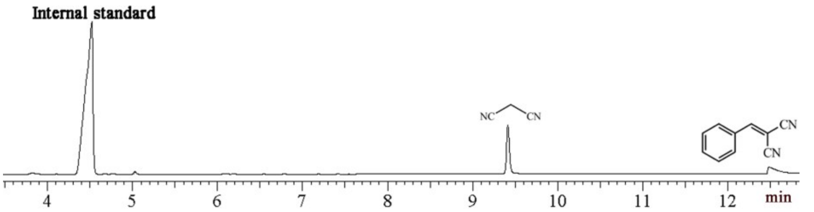
Internal standard
NC
CN
CN
CN
4
5
6
7
8
9
10
11
12
min

(g)

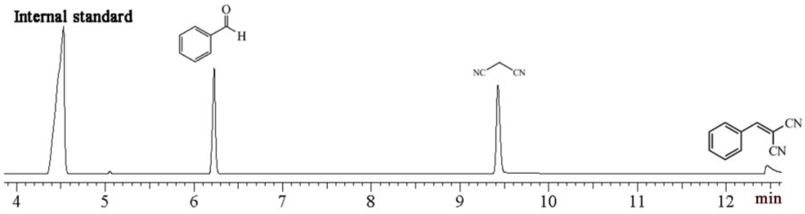
Internal standard
O
H
NC
CN
CN
CN
4
5
6
7
8
9
10
11
12
min

(h)

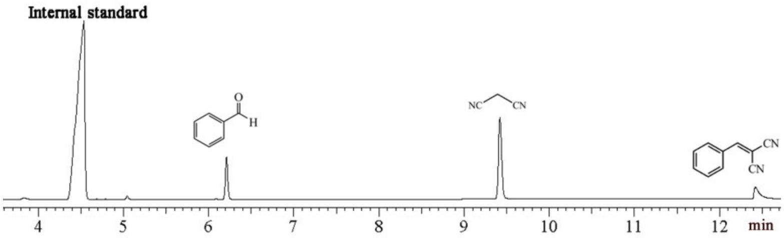
Internal standard
O
H
NC
CN
CN
CN
4
5
6
7
8
9
10
11
12
min

(i)

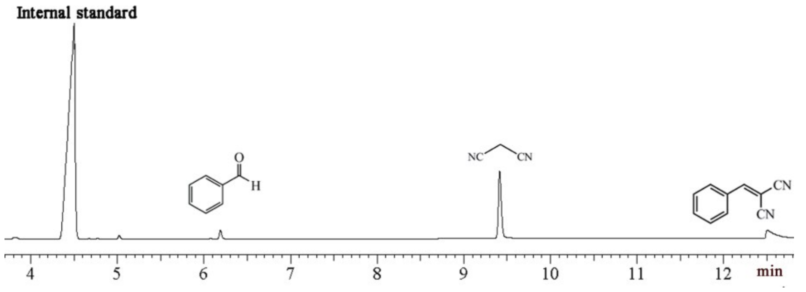
Internal standard
O
H
NC
CN
CN
CN
4
5
6
7
8
9
10
11
12
min

(j)

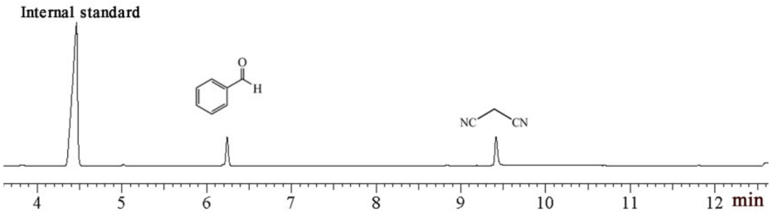
Internal standard
O
H
NC
CN
4
5
6
7
8
9
10
11
12
min

(k)

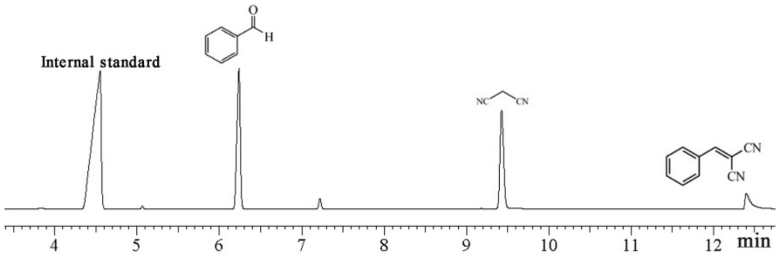

(l)

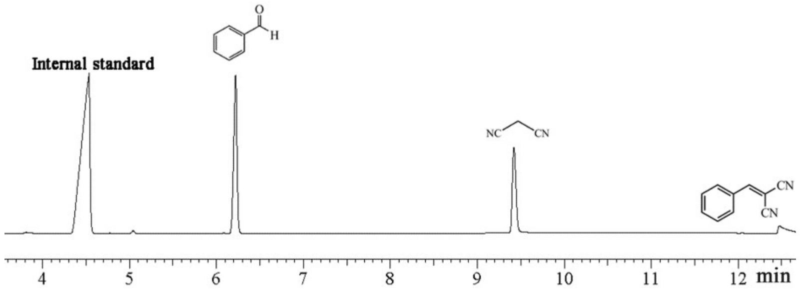

(m)

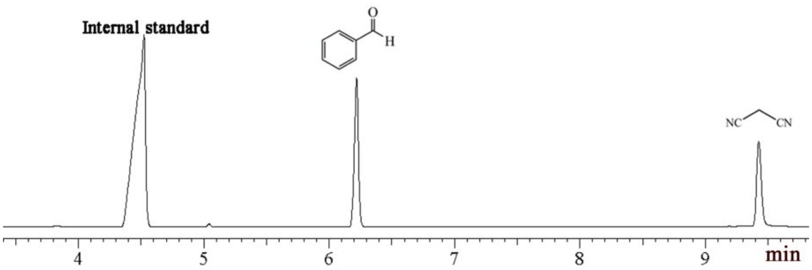

(n)

Fig. S13 GC of Knoevenagel condensation reaction.

(a) Malononitrile with benzaldehyde without catalyst after 1 h. (b) Malononitrile with benzaldehyde using catalyst $CdCl_2 \cdot 2.5H_2O$ after 1 h. (c) Malononitrile with benzaldehyde using catalyst **L** after 1 h. (d) Malononitrile with benzaldehyde using catalyst **2** (3mg) after 1 h. (e) Malononitrile with benzaldehyde using catalyst **2** (5mg) after 1 h. (f) Malononitrile with benzaldehyde using catalyst **2** (8mg) after 1 h. (g) Malononitrile with benzaldehyde using catalyst **2** (10mg) after 1 h. (h) Malononitrile with benzaldehyde using catalyst **2** after 1h at room temperature. (i) Malononitrile with benzaldehyde using catalyst **2** after 1h at 40°C. (j) Malononitrile with benzaldehyde using catalyst **2** after 1h at 50°C. (k) Malononitrile with benzaldehyde using catalyst **2** after 1h at 60°C in CH_3OH. (l) Malononitrile with benzaldehyde using catalyst **2** after 1h at 60°C in CH_3COCH_3. (m) Malononitrile with benzaldehyde using catalyst **2** after 1h at 60°C in CH_2Cl_2. (n) Malononitrile with benzaldehyde using catalyst **2** after 1h at 60°C in $C_6H_5CH_3$.

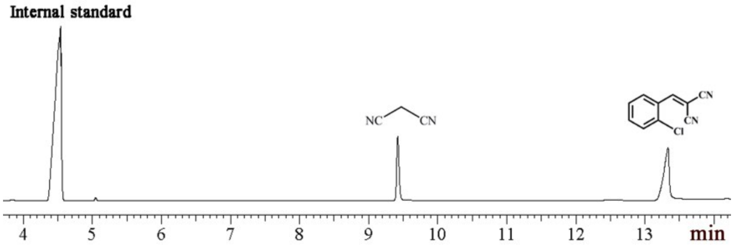

(a)

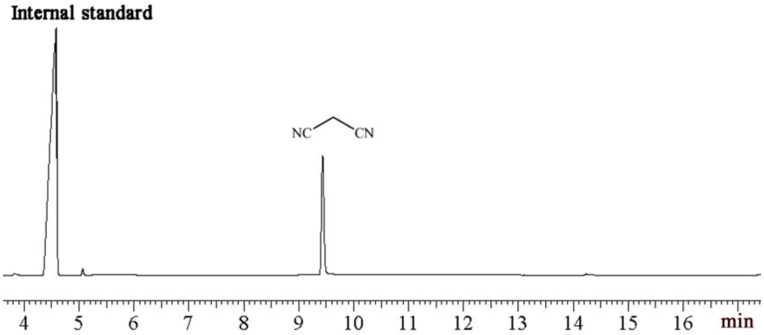

(b)

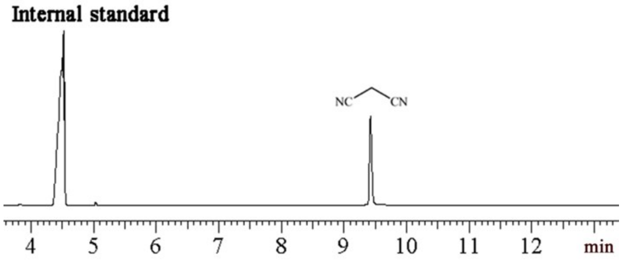

(c)

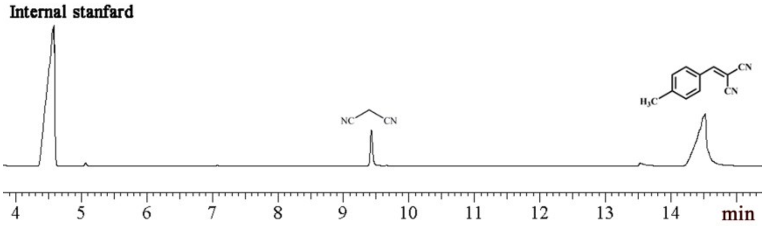

(d)

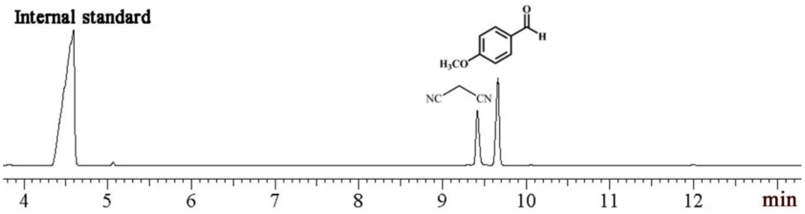

(e)

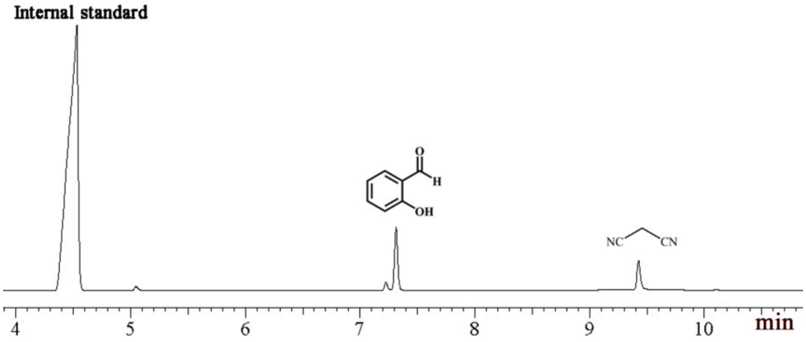

(f)

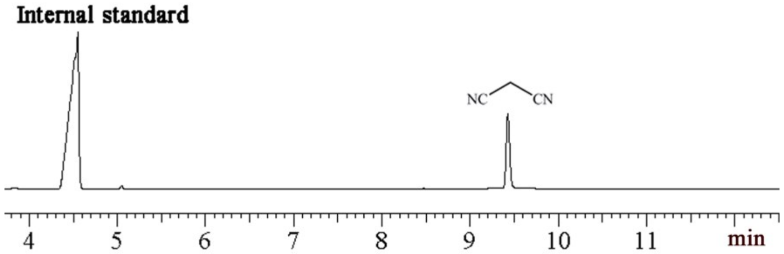

(g)

Fig. S14. The reactions of malononitrile with different benzaldehyde derivatives (a) Malononitrile with 2-chlorobenzaldehyde using catalyst **2** after 1 h. (b) Malononitrile with 4-cyanobenzaldehyde using catalyst **2** after 1 h. (c) Malononitrile with 4-nitrobenzaldehyde using catalyst **2** after 1 h. (d) Malononitrile with 4-methylbenzaldehyde using catalyst **2** after 1 h. (e) Malononitrile with 4-methoxybenzaldehyde using catalyst **2** after 1 h. (f) Malononitrile with salicylaldehyde using catalyst **2** after 1 h. (g) Malononitrile with 2-naphthaldehyde using catalyst **2** after 1 h.

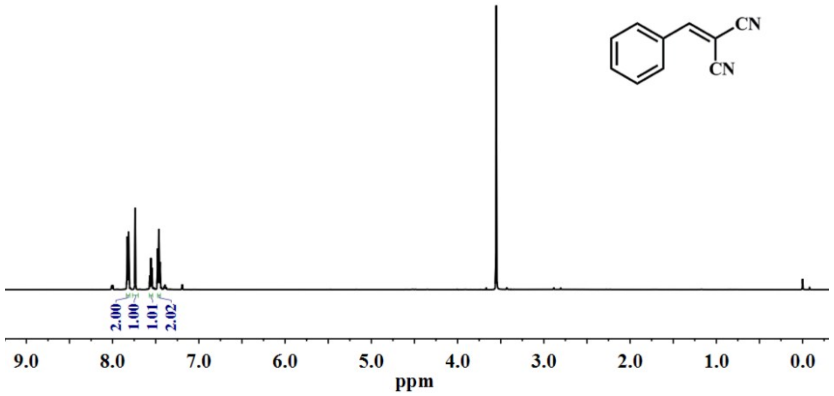
CN
CN
2.00
1.00
1.01
2.02
9.0
8.0
7.0
6.0
5.0
4.0
3.0
2.0
1.0
0.0
ppm

(a)

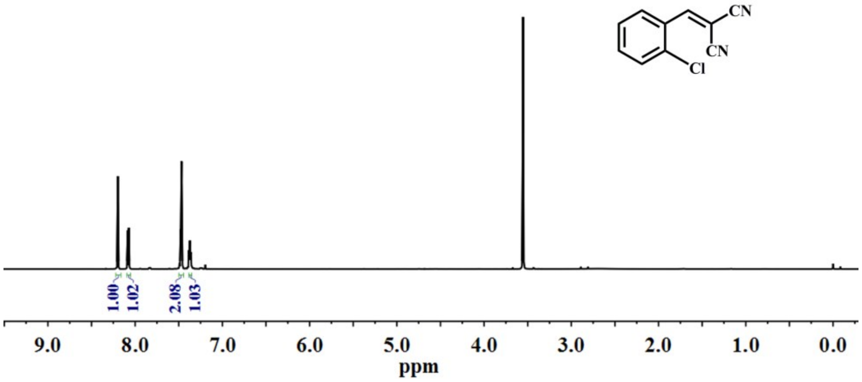
CN
CN
Cl
1.00
1.02
2.08
1.03
9.0
8.0
7.0
6.0
5.0
4.0
3.0
2.0
1.0
0.0
ppm

(b)

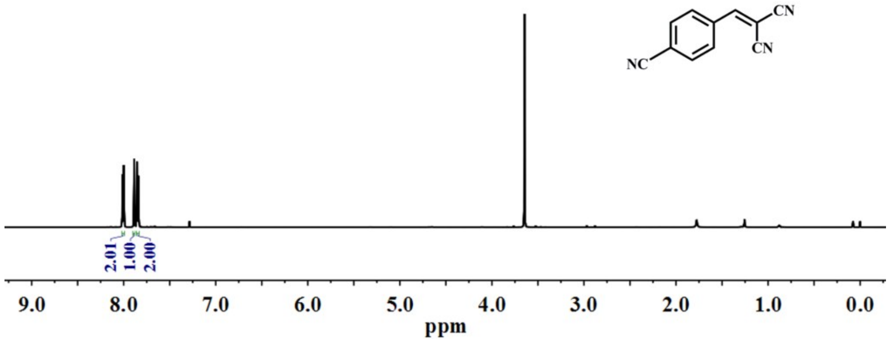
CN
CN
NC
2.01
1.00
2.00
9.0
8.0
7.0
6.0
5.0
4.0
3.0
2.0
1.0
0.0
ppm

(c)

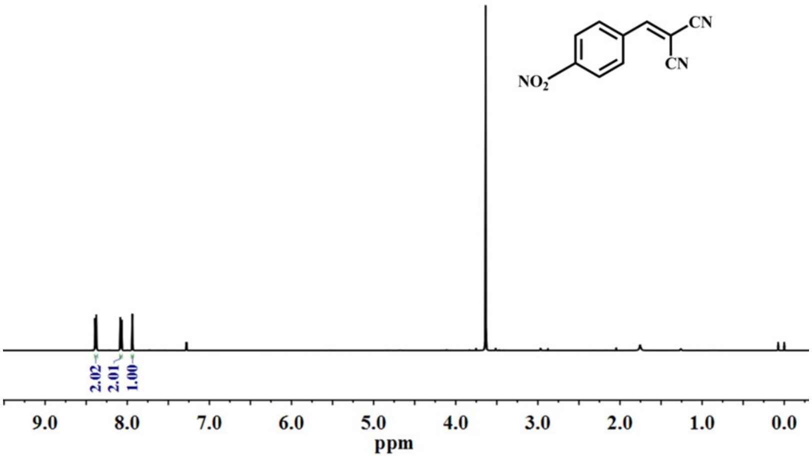
CN
CN
NO_2
2.02
2.01
1.00
9.0
8.0
7.0
6.0
5.0
4.0
3.0
2.0
1.0
0.0
ppm

(d)

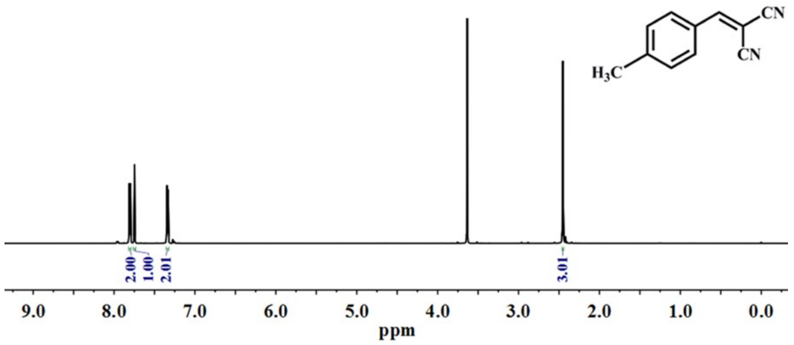
CN
CN
H3C
2.00
1.00
2.01
3.01
9.0
8.0
7.0
6.0
5.0
4.0
3.0
2.0
1.0
0.0
ppm

(e)

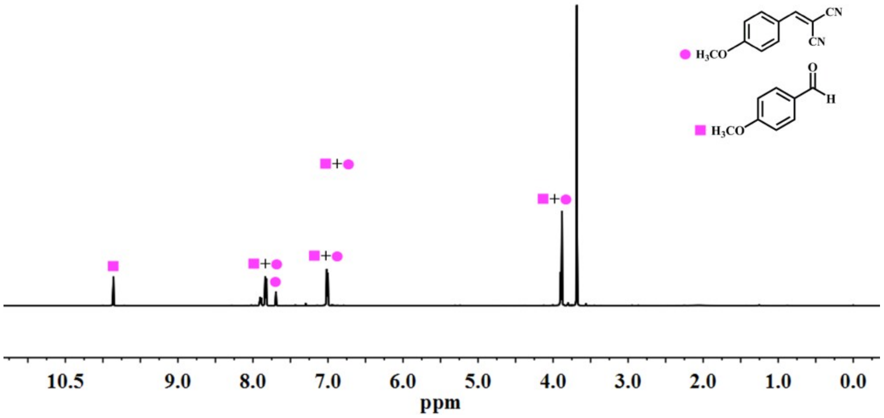
CN
CN
● H3CO
O
H
■ H3CO
■
■+●
●
■+●
■+●
■+●
10.5
9.0
8.0
7.0
6.0
5.0
4.0
3.0
2.0
1.0
0.0
ppm

(f)

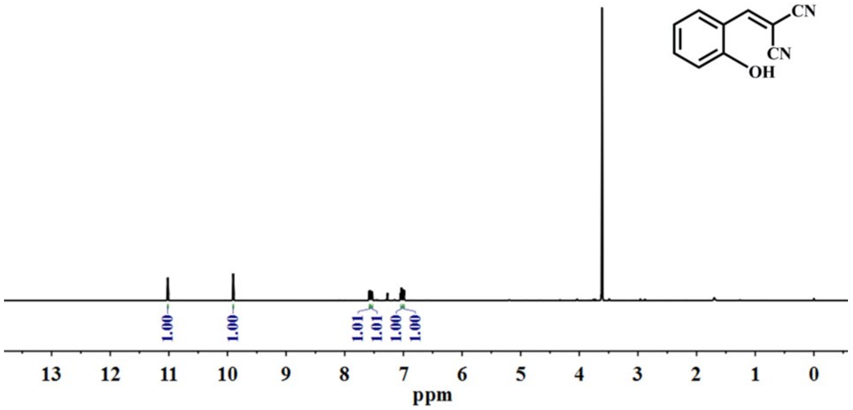
CN
CN
OH
1.00
1.00
1.01
1.01
1.00
1.00
13
12
11
10
9
8
7
6
5
4
3
2
1
0
ppm

(g)

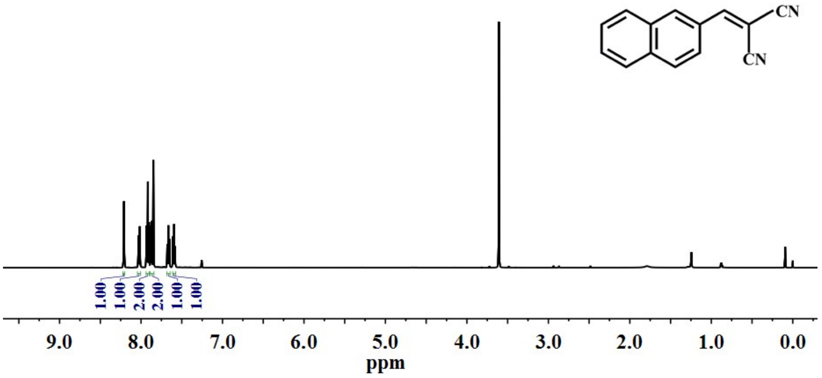
CN
CN
1.00
1.00
2.00
2.00
1.00
1.00
9.0
8.0
7.0
6.0
5.0
4.0
3.0
2.0
1.0
0.0
ppm

(h)

Fig. S15 ^{1}H and spectra of the crude products from the Knoevenagel condensation reaction of malononitrile with (a) Benzaldehyde. (b) 2-Chlorobenzaldehyde. (c) 4-cyanobenzaldehyde. (d) 4-nitrobenzaldehyde. (e) 4-methylbenzaldehyde. (f) 4-methoxybenzaldehyde. (g) salicylaldehyde. (h) 2-naphthaldehyde (The signal in the range of 3.5-4.0 ppm was caused by excessive malononitrile).

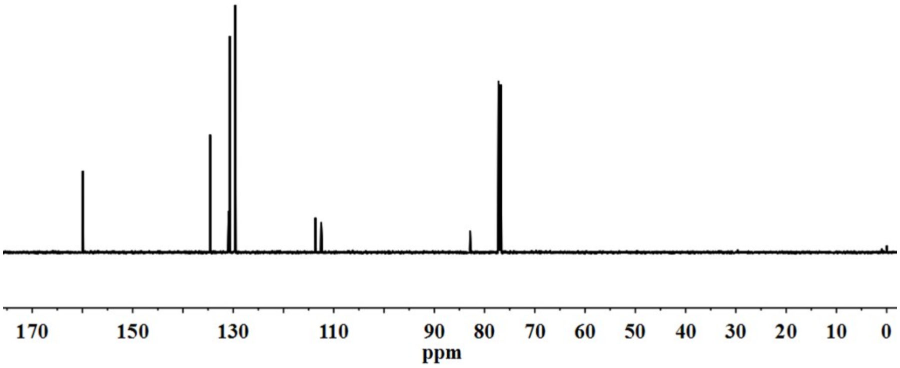

Fig. S16 ^{13}C NMR spectra (500 MHz, $CDCl_3$, TMS) for benzylidenemalononitrile: δ76.79, 77.21, 82.87, 112.50, 113.88, 129.80, 130.89, 130.91, 134.59, 159.90.

Table S4 The effects of time and catalysts on Knoevenagel condensation reaction.

Entry	Catalyst (mg)	Temperature (℃)	Time (min)	conversion(%) (with catalyst)	conversion(%) (without catalyst)
1	10	60	10	58	58
2			20	70	59
3			30	85	59
4			40	92	58
5			50	97	60
6			60	99	61

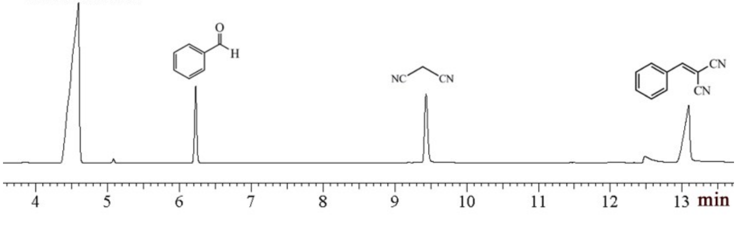

(a)

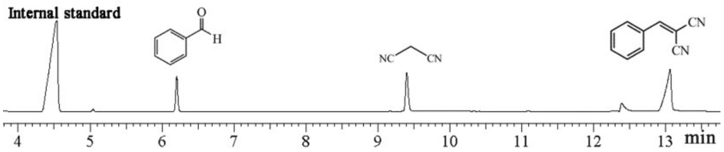

(b)

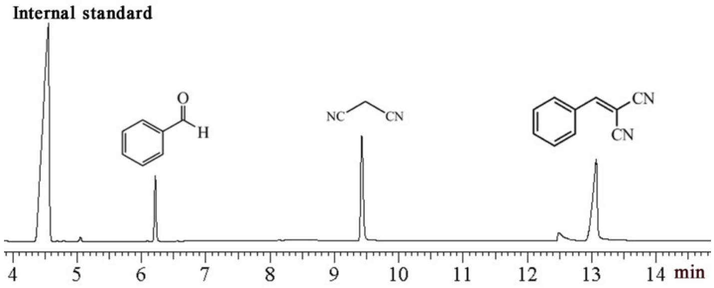

(c)

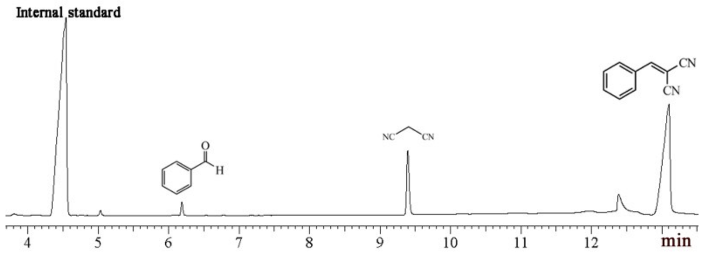

(d)

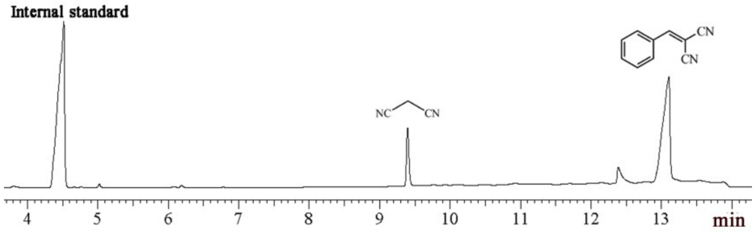

(e)

(f)

Fig. S17 GC spectra of catalytic reactions between the malononitrile and benzaldehyde at different reaction time. (a) Catalytic reaction for 10 minutes. (b) Catalytic reaction for 20 minutes. (c) Catalytic reaction for 30 minutes. (d) Catalytic reaction for 40 minutes. (e) Catalytic reaction for 50 minutes. (f) Catalytic reaction for 60 minutes.

By comparison of the IR spectra of **2** before and after the catalysis, there is a slight variation between them (Fig. S1 and Fig. S18). The peak at 648 cm^{-1} disappeared and a new peak at 618 cm^{-1} appeared, which indicates the structure of **2** has changed. The solid state UV-Vis spectrum of **2** indicates that a new absorption band around 315-375 nm appeared after catalysis, which also shows the structure of **2** has changed (Fig. S19).

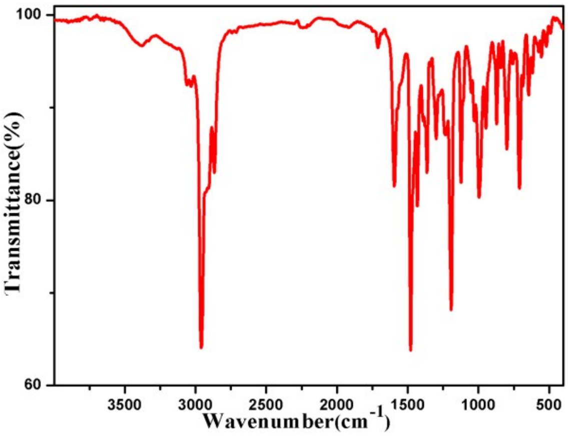

Fig. S18 FT-IR spectrum of **2** after catalytic reaction.

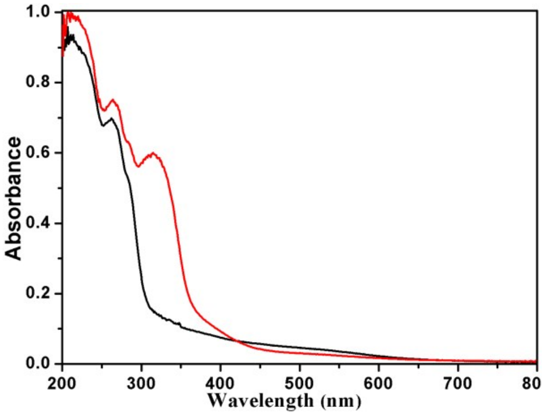

Fig. S19 Solid state UV-Vis spectra of **2** before (black) and after (red) catalytic reaction.